Invited paper for the
International Conference on the
Dynamical Properties of Heavy Ion Reactions
Johannesburg, S. Africa, 1-3 August 1978



# CENTRAL COLLISIONS OF RELATIVISTIC NUCLEI

Arthur M. Poskanzer



July 1978

Prepared for the U. S. Department of Energy
under Contract W-7405-ENG-48

Invited paper for the
International Conference on the
Dynamical Properties of Heavy Ion Reactions
Johannesburg, S.Africa, 1-3 August 1978

LBL-7762

# CENTRAL COLLISIONS OF RELATIVISTIC NUCLEI

Arthur M. Poskanzer

Lawrence Berkeley Laboratory
University of California
Berkeley, California 94720

## ABSTRACT

New data for relativistic heavy ion collisions are presented for the emitted protons and pions, and for the average multiplicities and angular correlations of the charged particles. Comparisons with several different theoretical approaches are made including the nuclear firestreak model. It appears that there is a group of nucleons with randomized motion and high temperature. The stage has been reached where one is beginning to look for effects due to the expansion of a compressed region.

The Bevalac is a combination of two accelerators. The first is the SuperHILAC, a linear accelerator for heavy ions up to 8.5 MeV/nucleon. The second is the Bevatron, a synchrotron whose output energy can be varied from 150 MeV/nucleon up to about 2 GeV/nucleon, that is, velocities ranging from 0.5 to 0.9 c. At present the heaviest projectile with good intensities for counter experiments is $^{40}Ar$. Emulsion and streamer chamber photos show that collisions of such relativistic nuclei with heavy target nuclei are extremely complicated with many charged particles emitted. What do we expect to learn from such horrendously complicated collisions? Our goal is to study nuclear matter at high density and temperature. Our experimental knowledge concerning nuclear matter consists of the equilibrium density of nuclei, the binding energy of nuclear matter, and recently some information about the compressibility. Nuclear matter at high density has not been studied although there are many speculations about pion condensates, density isomers, and quark matter.

Our experiment is a collaborative project [1] between LBL, GSI, and the University of Marburg. Our scattering chamber, which is shown in Fig. 1, is a 1-meter diameter sphere with 3-mm thick walls containing a $\Delta E$-$E$ telescope and surrounded by 80 plastic scintillators. The scintillators measure the associated multiplicity of charged particles of any kind above a low-energy threshold in coincidence with one fragment which is identified in the telescope and has its energy and angle measured. Therefore, we measure single particle inclusive spectra with associated multiplicity. The plastic scintillators are arranged into three azimuthal rings around the beam with a few additional scintillators at back angles. Thus the azimuthal correlation of charged particles can be obtained. The telescope inside the scattering chamber is shown in Fig. 2. It consists of two silicon ΔE detectors followed by 7 cm of Ge made up of two pieces backed by a reject detector. It measures positive pions from 20 to 100 MeV, protons from 5 to 200 MeV, deuterons up to 250 MeV, and tritons up to 300 MeV. Positive pions must be distinguished from the negative pions which are captured when they stop in the E detector. This is done by observing the delayed coincidence of the $\pi^+ \rightarrow \mu^+ \rightarrow e^+$ decay from the stopped positive pions with a 2.2 μsec mean life.

Previously we have compared our data to the nuclear fireball model [2,3]. This model assumes that the nuclei make clean cylindrical cuts through each other and the nucleons which are mutually swept out participate in forming the fireball. Kinematics allow one to calculate the forward velocity of the fireball and the energy in the fireball system. It is then assumed that the fireball is thermalized and decays as an ideal gas. The model has been extended to the firestreak model by Myers [4] by including a diffuse nuclear surface and gradients of the velocity and temperature across the fireball perpendicular to the beam direction. The firestreak calculations which will be presented here also include thermodynamic equilibrium [5,6] of the π, p, n, Δ and all the bound and unbound nuclear states up through mass five. A constant energy expansion up to a freezeout density of 0.12 hadrons/fm$^3$ is assumed. The two-body decay of the Δ and all unbound nuclear states is included. This model [7] predicts pions, nucleons, and light composite nuclei. Also multiplicities and spectator residues may be calculated. The model replaces the previously used fireball and coalescence [3,8] models. Although probably not the best model, it will be used as a standard model for making comparisons with all the data.

Our proton data from the 250 MeV/nucleon $^{20}Ne$ irradiation of U are shown in Fig. 3. Unfortunately they do not agree with our previously published data [3]. The slopes of the energy spectra are the same; however, the absolute normalization of the old data appears to have been a factor of 2.5 high at 60°, 90°, and 120°, and a factor of 3 high at 30°. The normalization of the old data involved an extrapolation to the evaporation region of the spectrum,and then normalization against a radiochemical cross section. The new data are normalized by counting directly the particles in the beam with a plastic scintillator. We apologize for the confusion caused by the incorrect normalization of the old data.

It can be seen in Fig. 3 that the firestreak calculation fits the new data fairly well at 90° and more backward angles. However, at forward angles, it predicts too much yield at low energies. In fact, our 20° spectrum is rising while the calculated curve is falling. To compare our data with other models which do not include composite particles, but only calculate the total nucleon charges emitted, we have summed

$$Z_i \; d^2\sigma/d(E/A)d\Omega \qquad (1)$$

for the new p, d, t data and the old $^{3,4}He$ data which were corrected for scattering and reaction loss and renormalized by the factors mentioned. The results are compared in Fig. 4 with the intranuclear cascade calculations [9,10] and two-fluid hydrodynamic calculations [10,11].

Agreement is good in both cases for these very different models. The 400 MeV/nucleon Ne plus U data are shown in Fig. 5. Again, the same qualitative discrepancy with the firestreak is seen. Siemens [12] in a recent simple analytical calculation has treated the expansion of the compressed fireball as an adiabatic expansion [13] up to the freezeout point. This model allows the fireball to cool as it expands because thermal energy is transformed into collective energy of radial expansion. In Fig. 6 it is seen that the qualitative effect of this is to move some of the low energy yield at forward angles to higher energies. Tentatively it appears to be in the right direction to bring better agreement with the data. The effect is most pronounced at forward laboratory angles because these represent the lowest energies in the fireball system which are most affected by the expansion velocity. The 90° spectrum is steeper because of the lower temperature. Sierk and Nix [14] have recently calculated the hydrodynamical expansion of a compressed sphere. They found that including the compressibility in the equation of state is quite important, but in the case they studied the results are not very sensitive to the actual value of the compressibility.

Our pion results are shown in Figs. 7 and 8. Yields from 2.1 GeV/nucleon Ne ions are about a factor of 50 higher than from 250 MeV/nucleon Ne ions. Although the yields predicted by the firestreak at 250 MeV/nucleon are reasonable, the experimental spectra are definitely more peaked. At 2.1 GeV/nucleon both the yields and shapes are in good agreement.

Another way to present the data is to make a contour plot as illustrated in Fig. 9. The abscissa of this plot is the rapidity.

It is a velocity-like variable defined as shown in the figure. It has the property that, in transforming to a moving system, one simply adds the rapidity of the system linearly. Nonrelativistically it approaches the velocity parallel to the beam in units of c. The ordinate is the perpendicular momentum divided by the mass of the particle. This is a relativistic invariant which nonrelativistically approaches the velocity perpendicular to the beam in units of c. Plotted as contours in the figure is the invariant cross section which is obtained from the previously illustrated double differential cross section simply by dividing by the momentum of the particle. Illustrated are three sets of contours obtained assuming isotropic emission in a moving system. The contours centered near zero rapidity represent particles from the target spectator and those centered near the beam rapidity, the projectile spectator. Contours centered at an intermediate rapidity and extending out to high perpendicular momentum represent the participants where the effects of high density and temperature are most likely to be found. In the case of an equal mass target and projectile there must be symmetry about the mean rapidity of the beam and target. In Fig. 10 for 400 MeV/nucleon $^{20}$Ne plus U, it can be seen that at low perpendicular momentum the contours center near the rapidity of the target, but at high perpendicular momentum they tend to center more near the intermediate rapidity region. Such plots are a more model-independent way of assessing the various contributing sources to the experimental data.

Now let us look at the information which can be obtained from the 80 plastic scintillators surrounding the outside of the scattering chamber. We record which scintillators have fired for each event recorded in the telescope. Three such events are shown in Fig. 11. The top event, with a few charged particles on the opposite side of the beam from the telescope, clearly resulted from a peripheral collision. The middle event, with a high multiplicity symmetrically distributed, clearly resulted from a central collision. The bottom asymmetric event may be associated with a type of hot spot. To obtain average multiplicities associated with different particles in the telescope, the data are corrected for double firing of the scintillators, accidentals, dead time, missing azimuthal angle, and are then integrated over polar angle. In presenting these average multiplicities from many different target-projectile combinations, it is convenient to plot them against a variable which is the average number of proton participants in the fireball geometry. This is given by [15]

$$\frac{\pi\, r_0^2\, (Z_t A_p^{2/3} + A_p A_t^{2/3})}{\pi\, r_0^2\, (A_p^{1/3} + A_t^{1/3})^2} \qquad (2)$$

The numerator consists of the number of protons in the target times the area of the projectile, plus the number of protons in the projectile times the area of the target. The denominator is the geometrical reaction cross section. In Fig. 12 the average multiplicities observed for four different projectile energies are shown. Interestingly, the data are approximately linear in this variable. However, they deviate considerably from the fireball geometry predictions at the higher projectile energies. Let us examine these deviations for the Ne plus U cases in Fig. 13. The four squares labeled "paddles" are the multiplicities at the four bombarding energies from the previous figure. The horizontal line labeled "fireball" corresponds to the solid lines in the previous figure. Actually the fireball curve should be raised slightly for pion production which would then be compensated for somewhat by composite particle formation. Also at low projectile energies the curve would turn over if absorption in the wall of the scattering chamber were taken into account. The curve labeled "firestreak" was obtained from the calculation previously described [7] by integrating over particles with sufficient energy to penetrate the wall of the scattering chamber. For the firestreak model this cut-off is more important in determining the increase of multiplicity with projectile energy than the inclusion of pions and composites.

Another way to calculate multiplicities is from the telescope data by taking the total single particle cross section divided by the geometric reaction cross section. To do this we remove the requirement of the E-reject counter from the telescope in order to integrate the charged particles out to all energies. They were then integrated over all angles and divided by a reaction cross section of 4.1 barns. The results are shown as the three triangles which agree quite well with the firestreak calculations.

What is the difference between the two ways of calculating the multiplicities? From the integration of the single particle cross sections we calculate multiplicities; but from the 80 paddles we calculate <u>associated</u> multiplicites. Just requiring a high energy proton at 90° in the telescope biases the paddle multiplicities to quite high values. Clearly, requiring a high energy proton at a large angle to the beam is equivalent to selecting a high multiplicity or a central collision.

Finally, let us look at the azimuthal correlation of charged particles relative to a proton in the telescope at an angle of 90° to the beam. The curves in Fig. 14 are for the three azimuthal rings of paddles. The $\phi$ angles of 0°, 180°, and 360° are in the plane of the telescope. The peak in the left-hand curve means that when a proton is observed in a telescope at 90° to the beam there is a positive correlation for observing charged particles on the opposite side of the beam line at a small angle to the beam. This is what one would call quasi-free scattering and is not at all unreasonably for this case of 1 GeV incident protons. The peaks in the other two curves at azimuthal angles of 180° for larger angles to the beam are not understood. It can be seen that for incident He ions the quasi-free peak disappears and the other peaks are also almost gone. For all heavier projectiles no peaks are observed. This indicates a considerable degree of azimuthal randomization, even though the correlation is expected to decrease with multiplicity.

In conclusion we can say that we have seen yield in the intermediate rapidity region where the nucleons have lost memory of whether they came from the target or projectile, that there appears to be a considerable degree of randomization, that the temperatures are quite high, and that we are beginning to look for effects in the data due to the expansion of a compressed region. We are about to start examining the single particle inclusive cross sections selected for high multiplicity. Although very different theories give similar results when integrated over impact parameter, the differences between theories are enhanced when selected for zero impact parameter collisions. Thus with the present more accurate data selected for high multiplicities we hope to begin to differentiate between the models. In fact, recently there is both lots of new experimental data and tremendous theoretical activity. Rapid progress in this field can be expected.


ACKNOWLEDGMENTS

I would like to acknowledge the indispensable collaboration in this work of Hans Gutbrod, Chuck King, George King, Bill Meyer, Nguyen Van Sen, Andres Sandoval, Reinhard Stock, and Kevin Wolf. For the firestreak calculations I would like to thank Jean Gosset, Joe Kapusta, and Gary Westfall. Permission to use some of the material of Ray Nix and the calculations of Phil Siemens, Y. Yariv and Zeev Fraenkel is appreciated. The support of Herman Grunder and the staff of the Bevalac is greatly appreciated.

This work was done with support from the Division of Physical Research of the U.S.Department of Energy, from the Bundesministerium für Forschung und Technologie, West Germany, and from the Gesellschaft für Schwerionen Forschung, Darmstadt, West Germany.

## REFERENCES

[1] J.Gosset, H.H.Gutbrod, J.-C.Jourdain, C.H.King, G.King, Ch.Lukner, W.G.Meyer, Nguyen Van Sen, A.M.Poskanzer, A.Sandoval, R.Stock, G.D.Westfall, and K.L.Wolf, unpublished (1978).

[2] G.D.Westfall, J.Gosset, P.J.Johansen, A.M.Poskanzer, W.G.Meyer, H.H.Gutbrod, A.Sandoval, and R.Stock, Phys. Rev. Letters 37 (1976) 1202.

[3] J.Gosset, H.H.Gutbrod, W.G.Meyer, A.M.Poskanzer, A.Sandoval, R.Stock, and G.D.Westfall, Phys. Rev. C 16 (1977) 629.

[4] W.D.Myers, Nucl. Phys. A 296 (1978) 177.

[5] A.Mekjian, Phys. Rev. Letters 38 (1977) 640; and Phys. Rev. C 17 (1978) 1051.

[6] J.I.Kapusta, Phys. Rev. C 16 (1977) 1493.

[7] J.I.Kapusta, G.D.Westfall, and J.Gosset, Phys. Rev. C (to be published, 1978).

[8] H.H.Gutbrod, A.Sandoval, P.J.Johansen, A.M.Poskanzer, J.Gosset, W.G.Meyer, G.D.Westfall, and R.Stock, Phys. Rev. Letters 37 (1976) 667.

[9] Z.Fraenkel and Y.Yariv, unpublished (1978).

[10] A.A.Amsden, J.N.Ginocchio, F.H.Harlow, J.R.Nix, M.Danos, E.C.Halbert, and R.K.Smith,Jr., Phys. Rev. Letters 38 (1977) 1055.

[11] A.A.Amsden, A.S.Goldhaber, F.H.Harlow, and J.R.Nix, Phys. Rev. C 17 (1978) 2080.

[12] P.Siemens, private communication (1978).

[13] J.P.Bondorf, S.I.A.Garpman, and J.Zimanyi, Nucl. Phys. A<u>296</u> (1978) 320.

[14] A.J.Sierk and J.R.Nix, private communication (1978).

[15] J.Hüfner and J.Knoll, Nucl. Phys. A<u>290</u> (1977) 460.

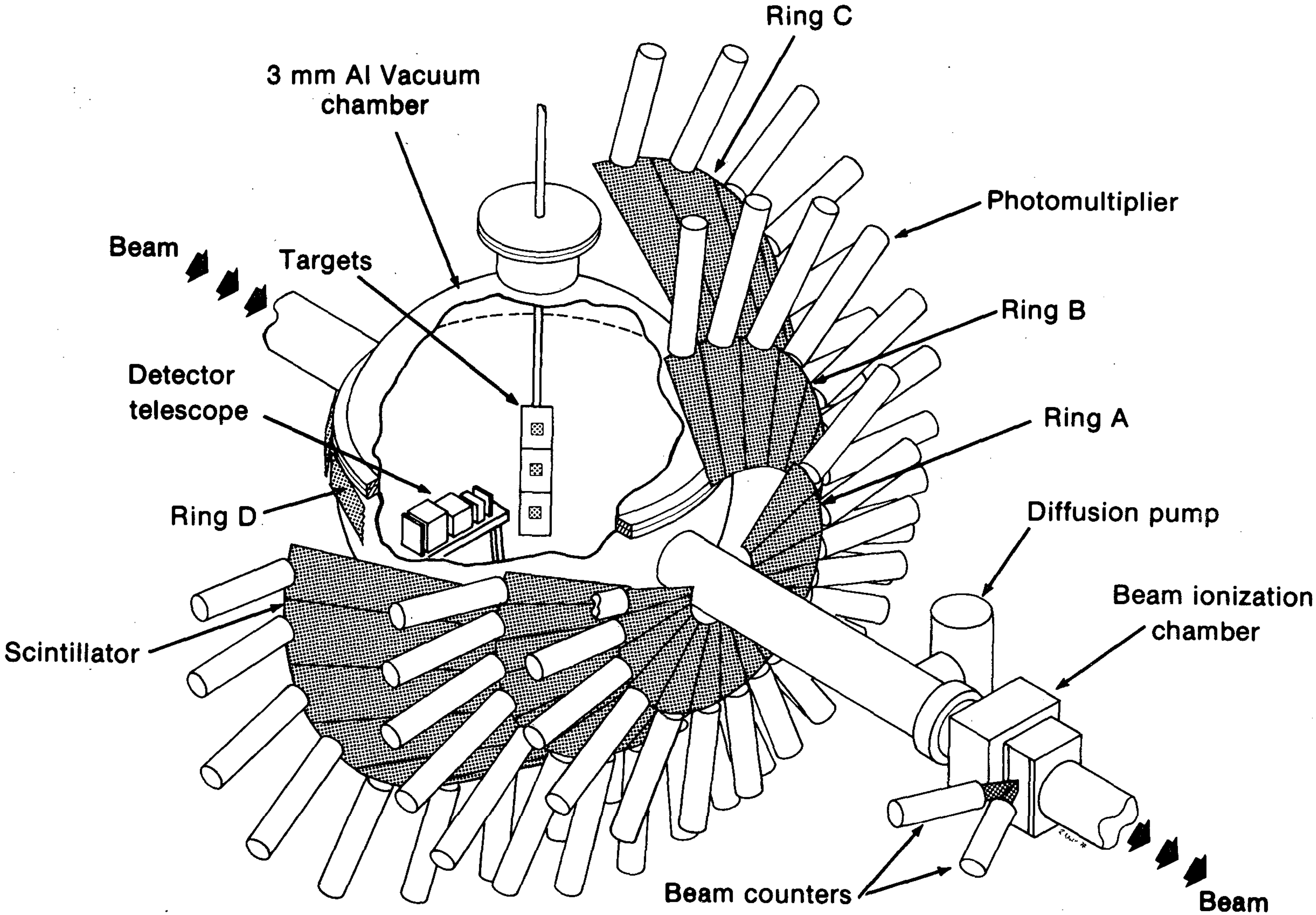


Fig. 1. Schematic diagram of the 1-meter-diameter spherical scattering chamber containing the silicon-germanium telescope and surrounded by the 80 plastic scintillators. XBL 782-7229C

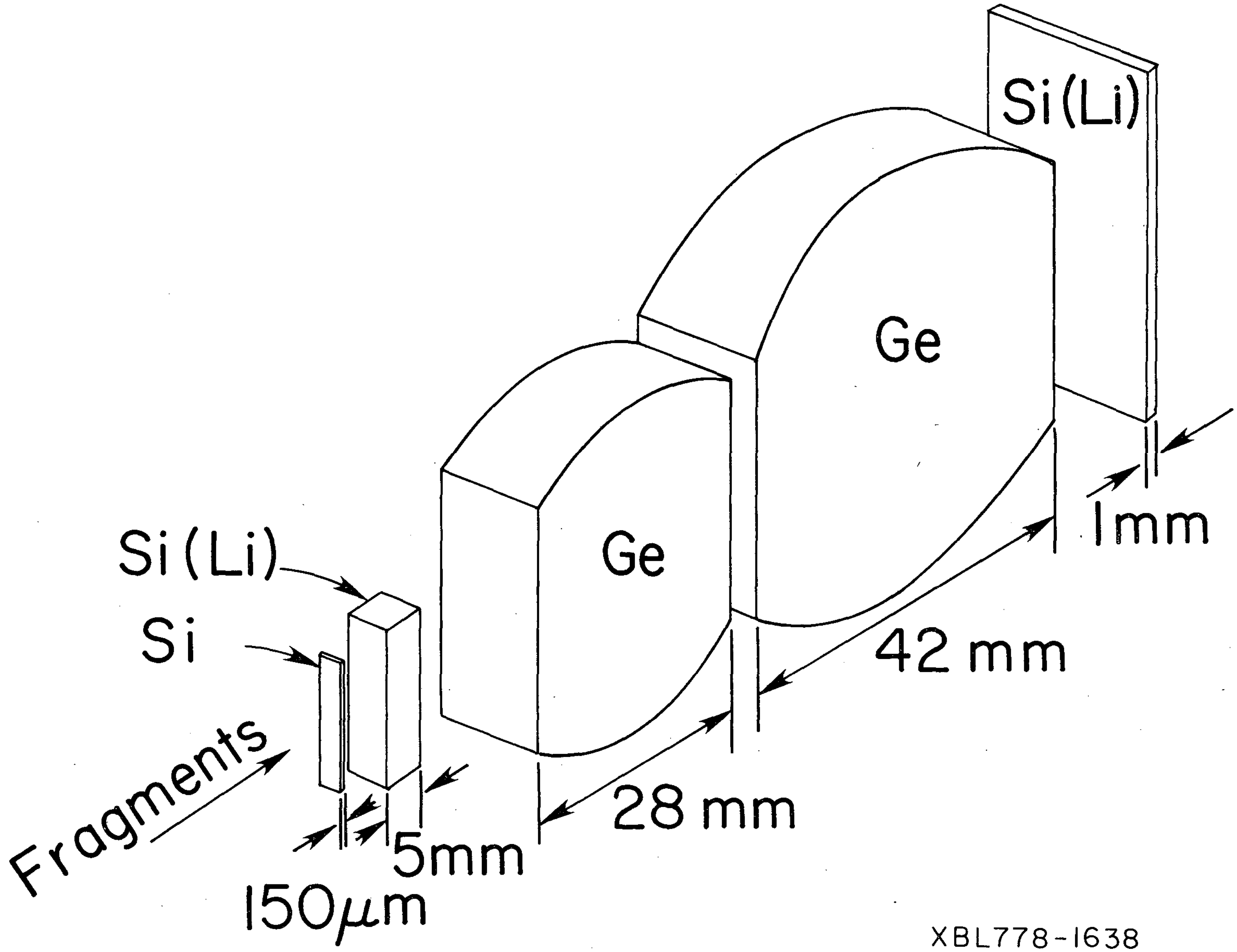


Fig. 2. The silicon-germanium telescope used for measuring the spectra of positive pions, protons, deuterons, and tritons.

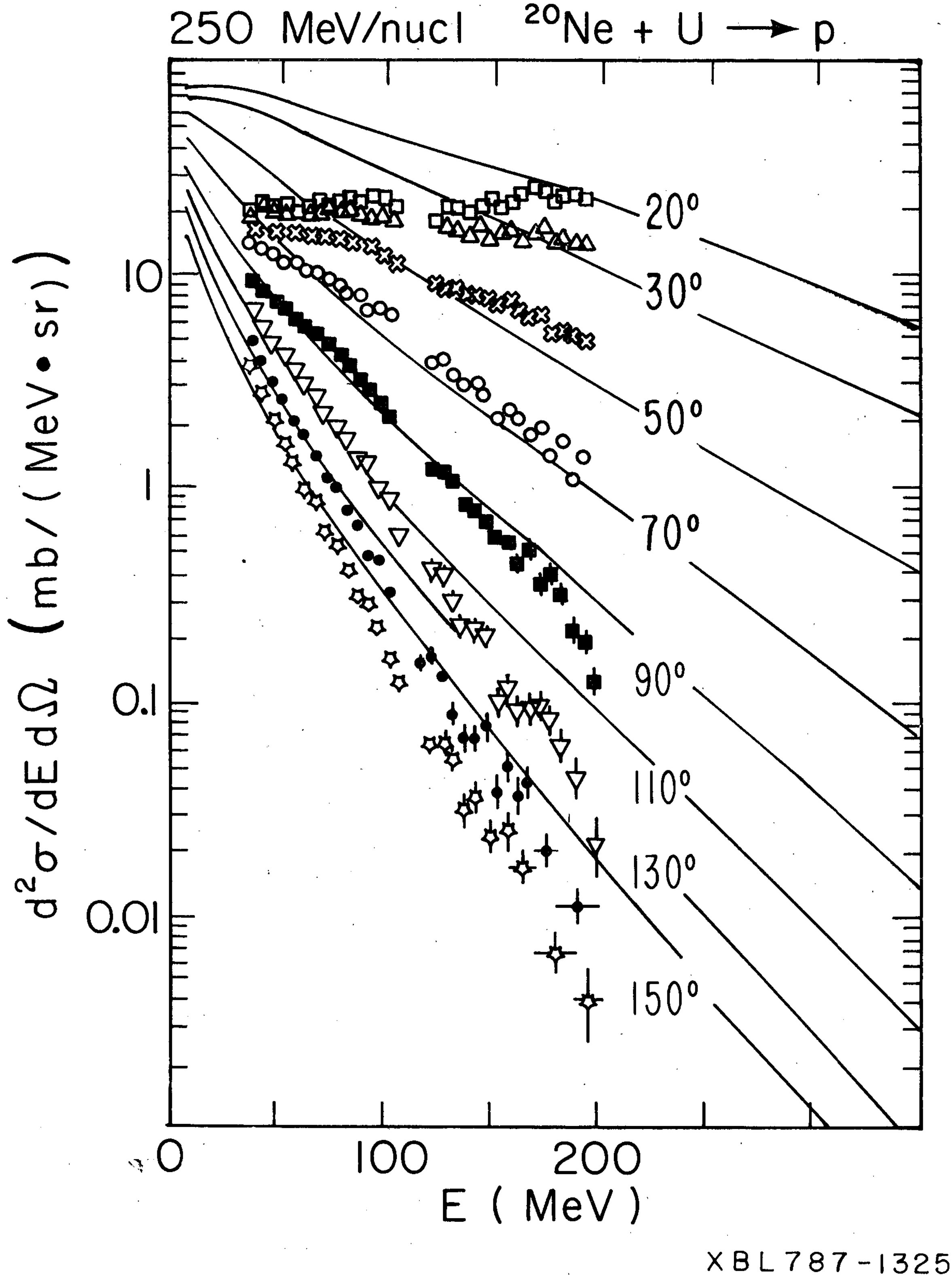


Fig. 3. Laboratory energy spectra at many angles to the beam for protons produced by 250 MeV/nucleon $^{20}$Ne ions on U. The solid curves are the firestreak calculation [7].

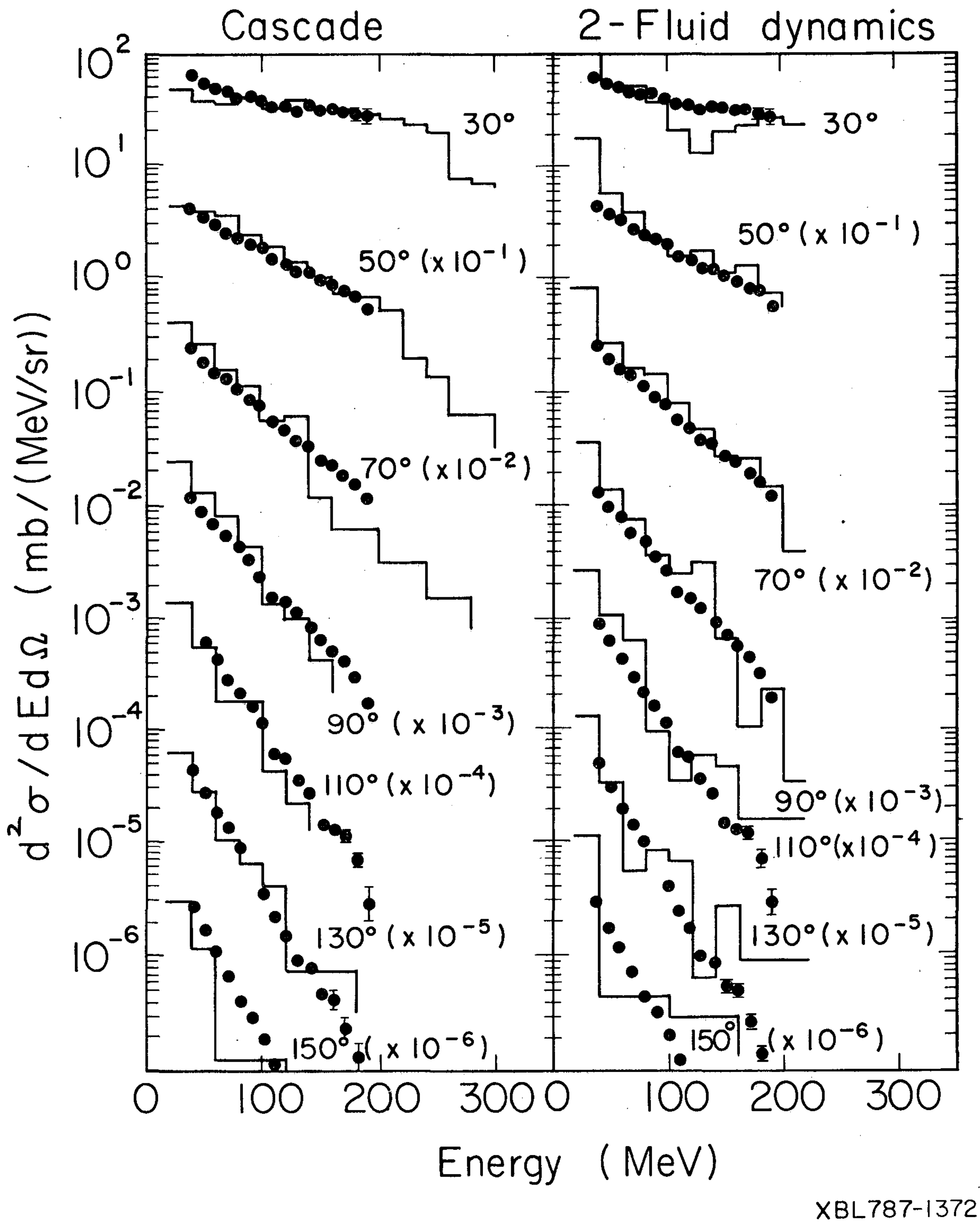


Fig. 4. The reaction of 250 MeV/nucleon $^{20}$Ne ions on U. The dots represent the emitted nucleon charges obtained by summing the present p, d, t data and the old $^{3,4}$He data [3]. The histograms are the calculations based on the models of the intranuclear cascade [9], and two-fluid dynamics [11].

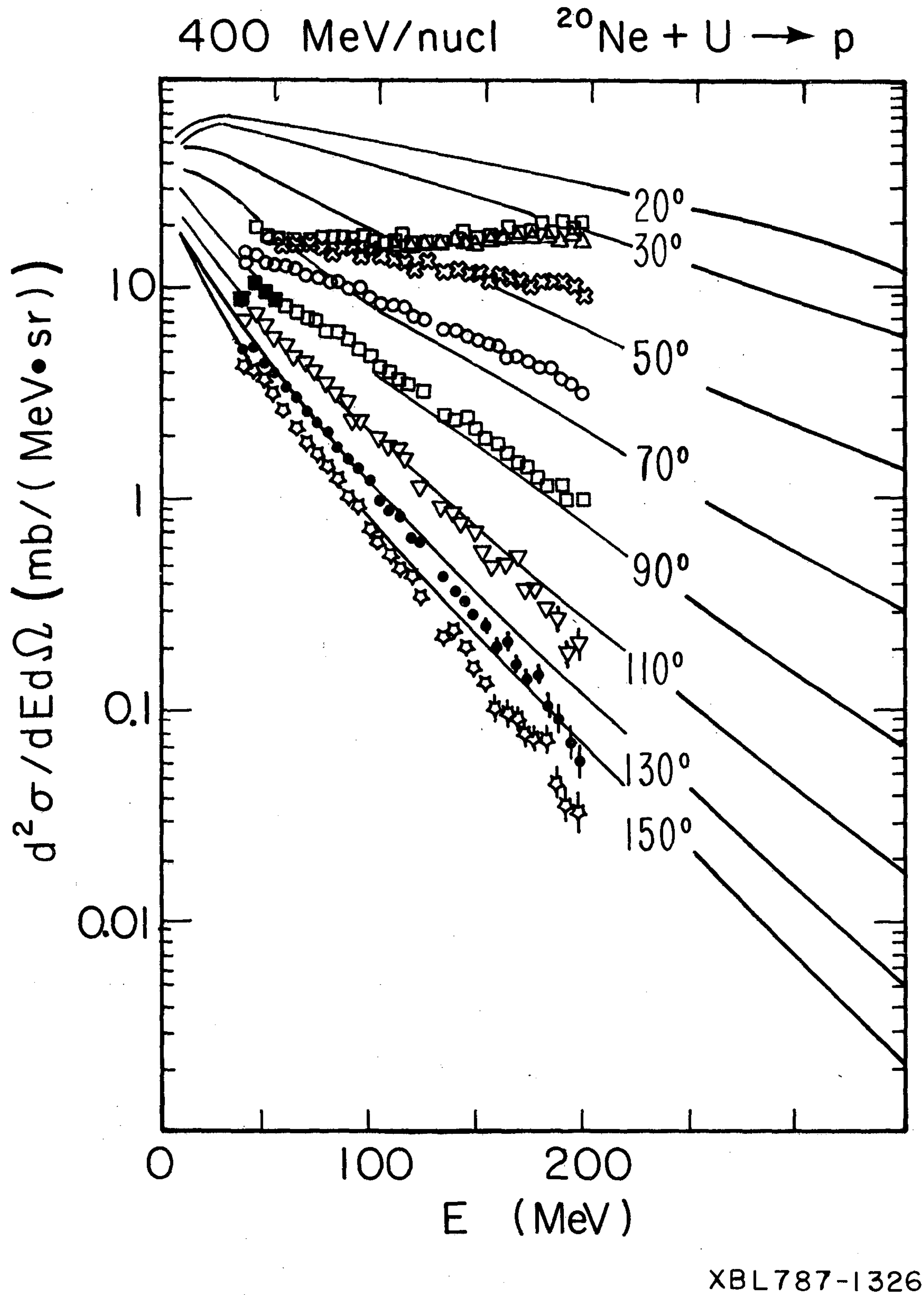


Fig. 5. Proton spectra from the interaction of 400 MeV/nucleon $^{20}$Ne ions with U. Solid curves are from the firestreak calculation [7].

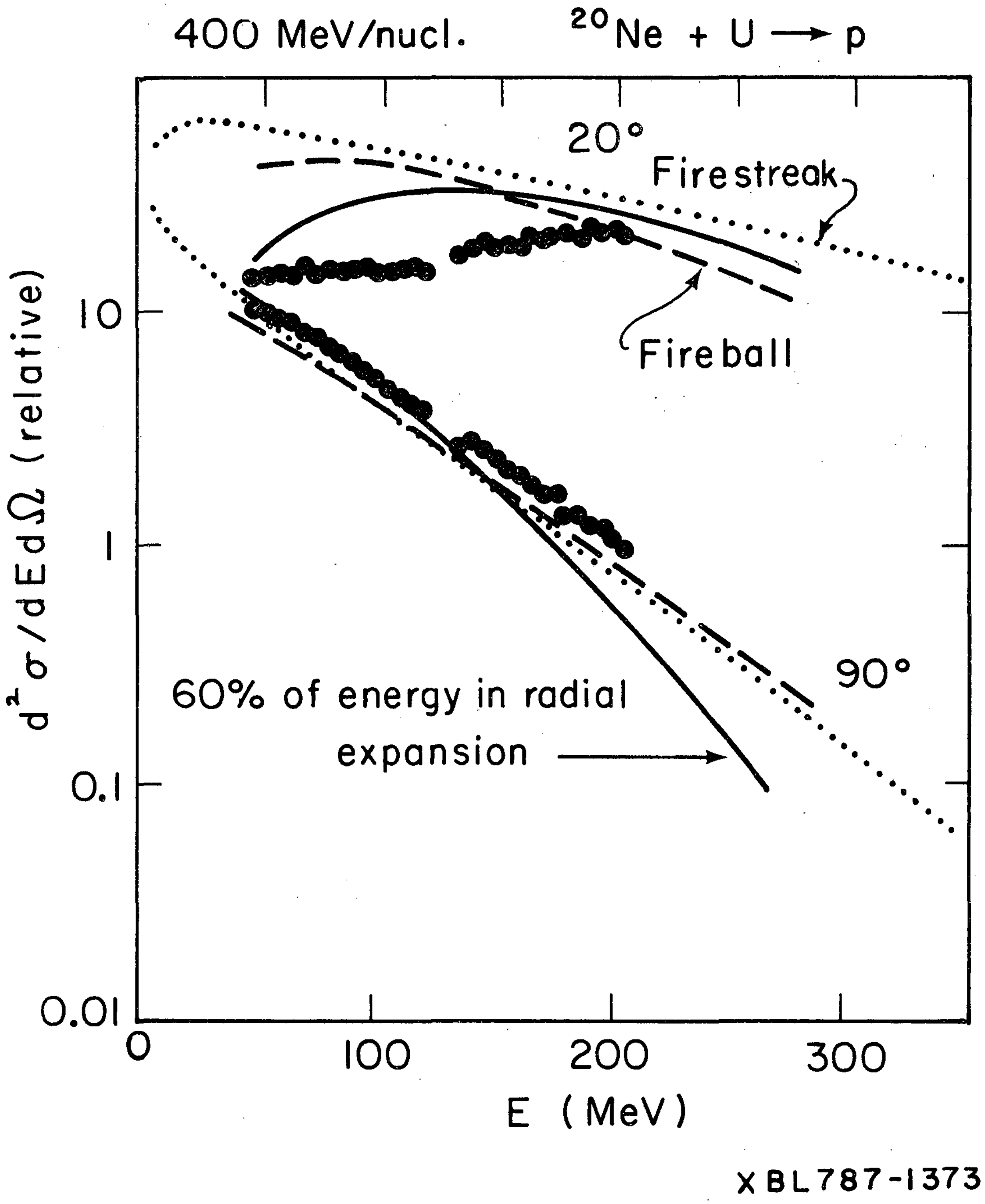


Fig. 6. The results of a calculation assuming the adiabatic expansion of a compressed fireball [12] (solid). Also shown are fireball (dashed) and firestreak (dotted) calculations. The points represent the proton data. All the curves have been normalized together at 90° to display the differences at 20°.

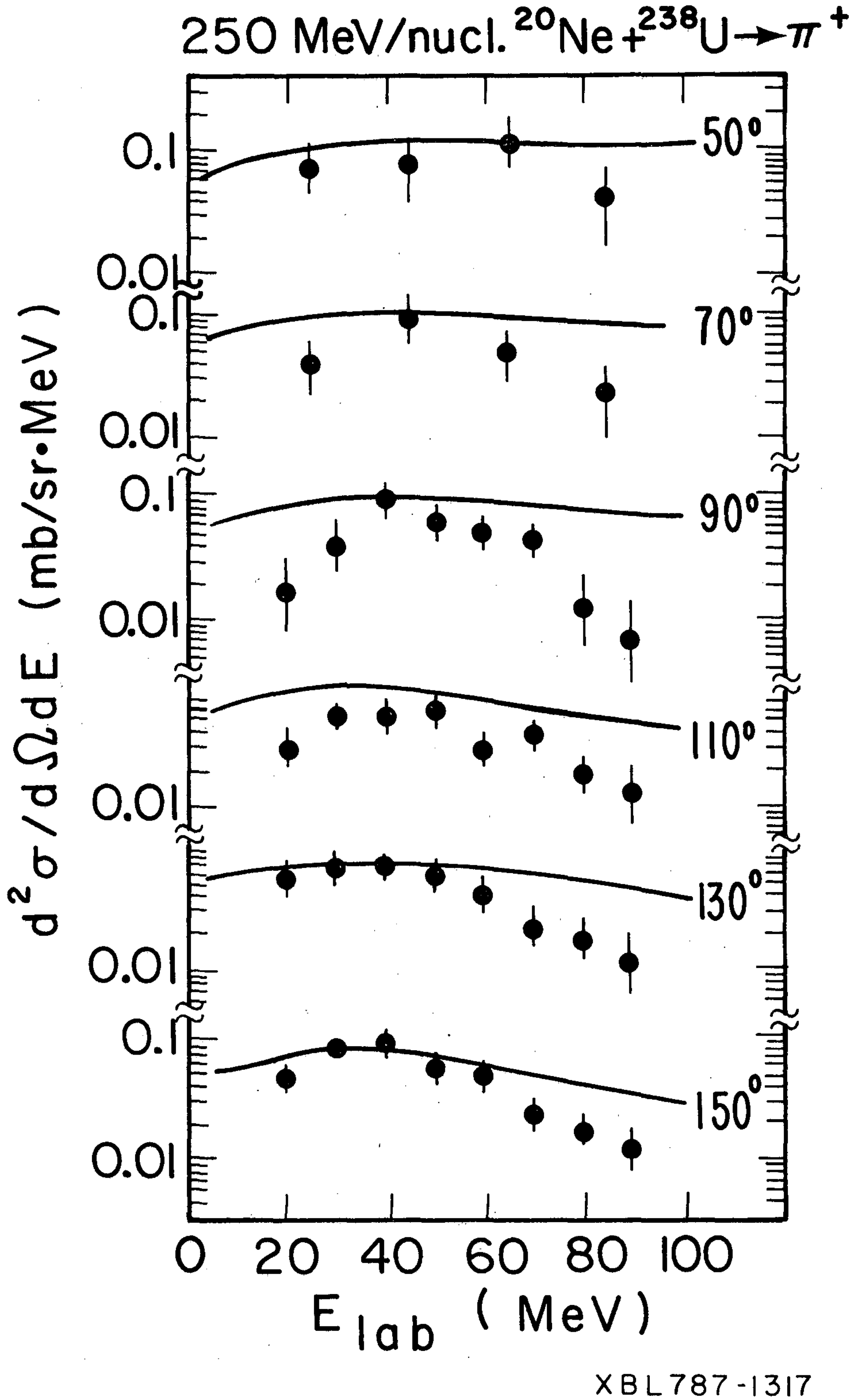


Fig. 7. Energy spectra at various angles to the beam for positive pions produced by 250 MeV/nucleon $^{20}$Ne ions on U. Solid curves are from the firestreak calculation [7].

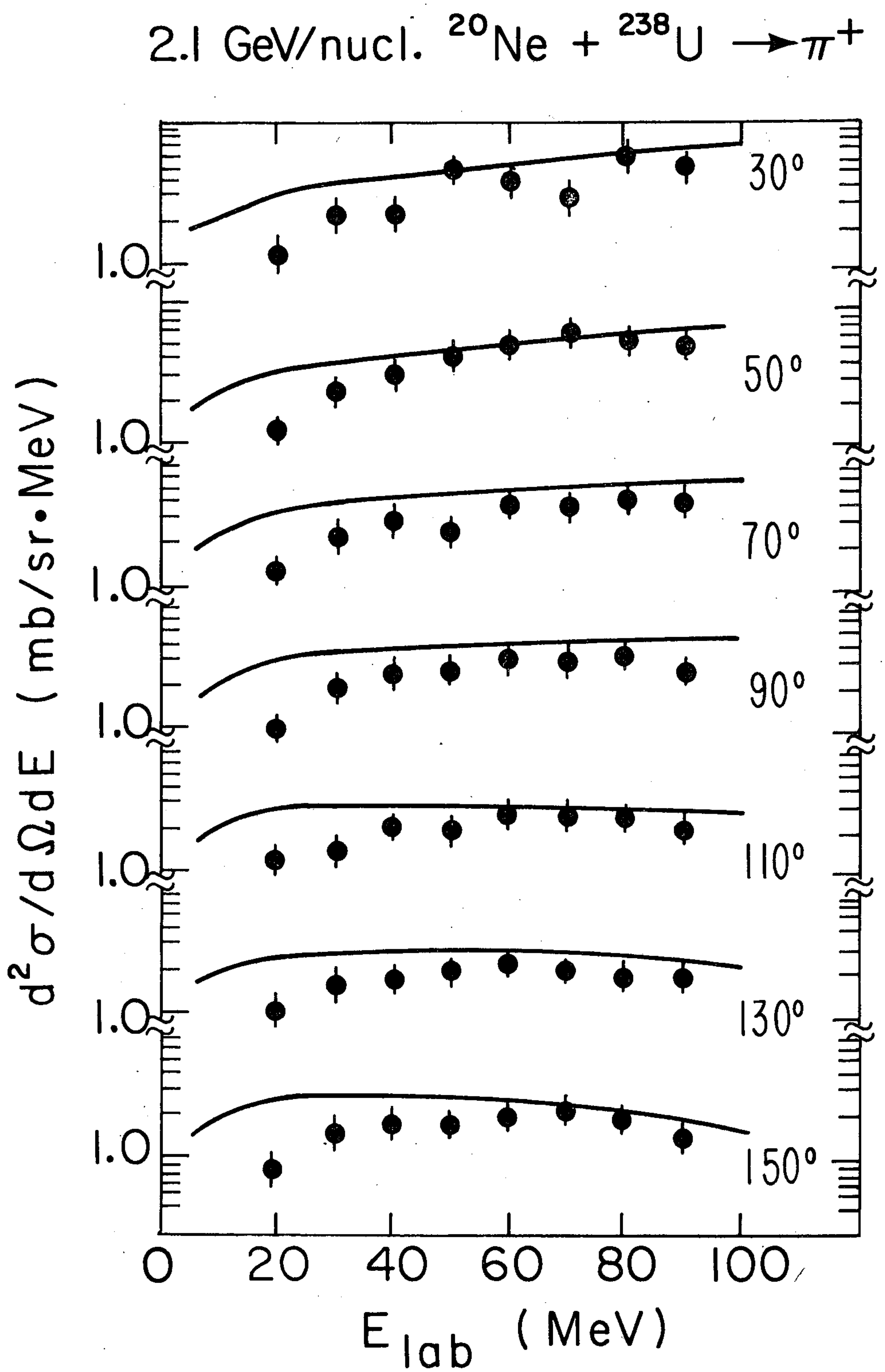


XBL 787-1318

Fig. 8. Energy spectra at various angles to the beam for positive pions produced by 2.1 GeV/nucleon $^{20}$Ne ions on U. Solid curves are from the firestreak [7].

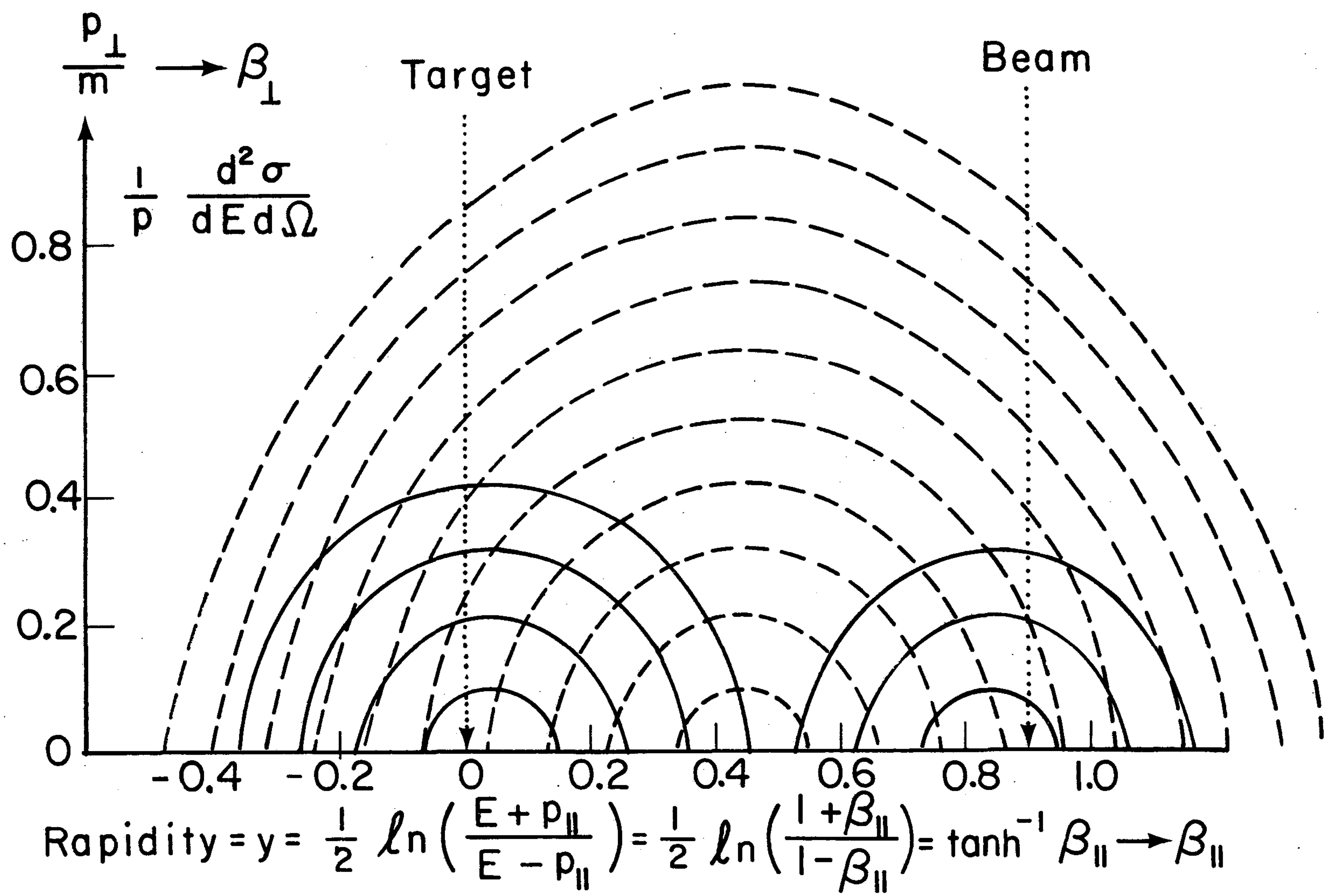


Fig. 9. Schematic contour plots of invariant cross section vs. rapidity and perpendicular momentum/mass of the particle. The contours are drawn in equal intervals of momentum for systems moving at three different rapidities. They are meant to represent the projectile fragments, the target fragments, and the intermediate rapidity region.

(XBL 787-1315)

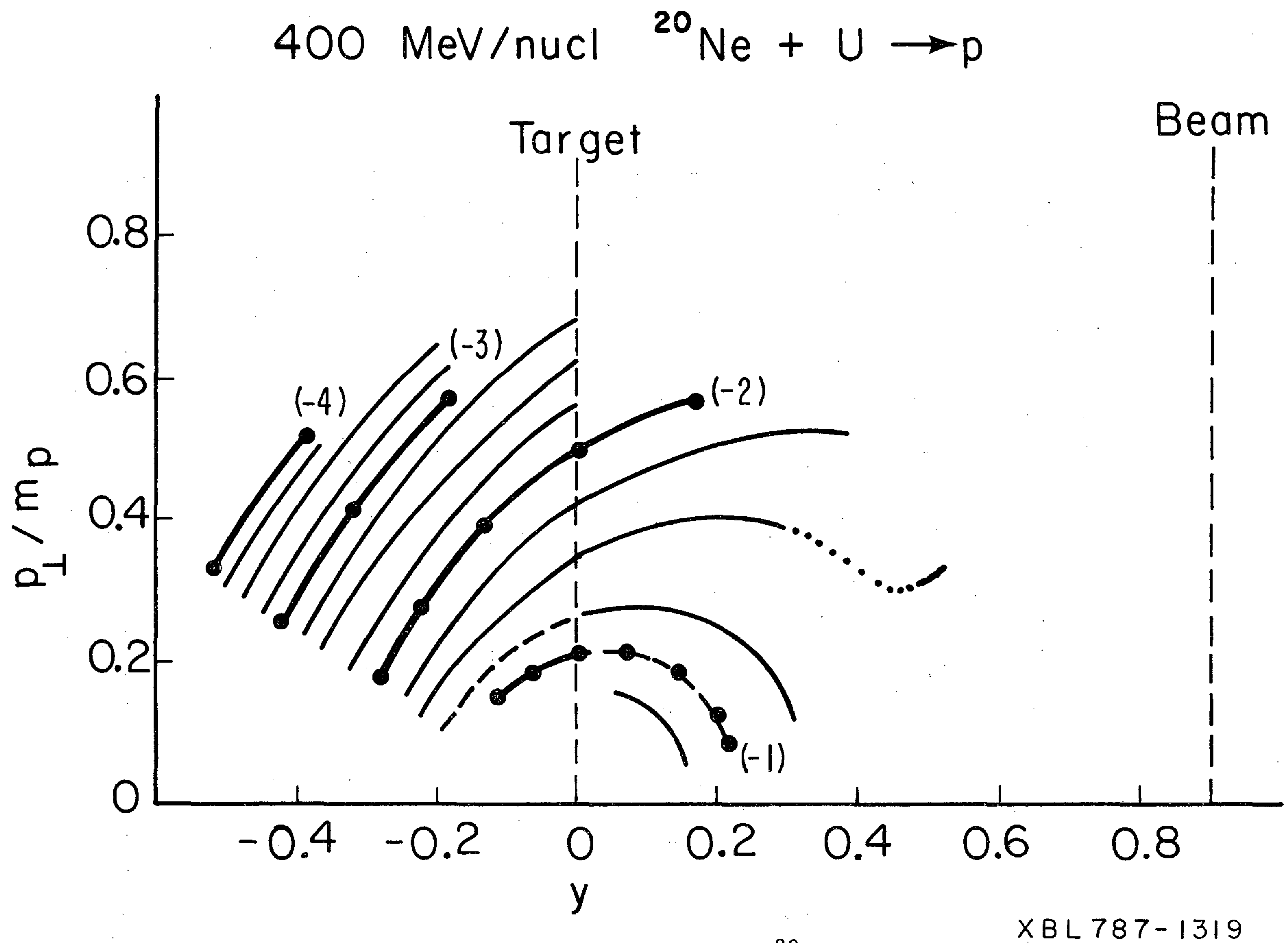


Fig. 10. Contour plot for protons from 400 MeV/nucleon $^{20}$Ne ions on U. There are four contours per decade. For the heavier curves with points, the logarithm of the invariant cross section is indicated in parentheses. The dashed curves are interpolations of the data.

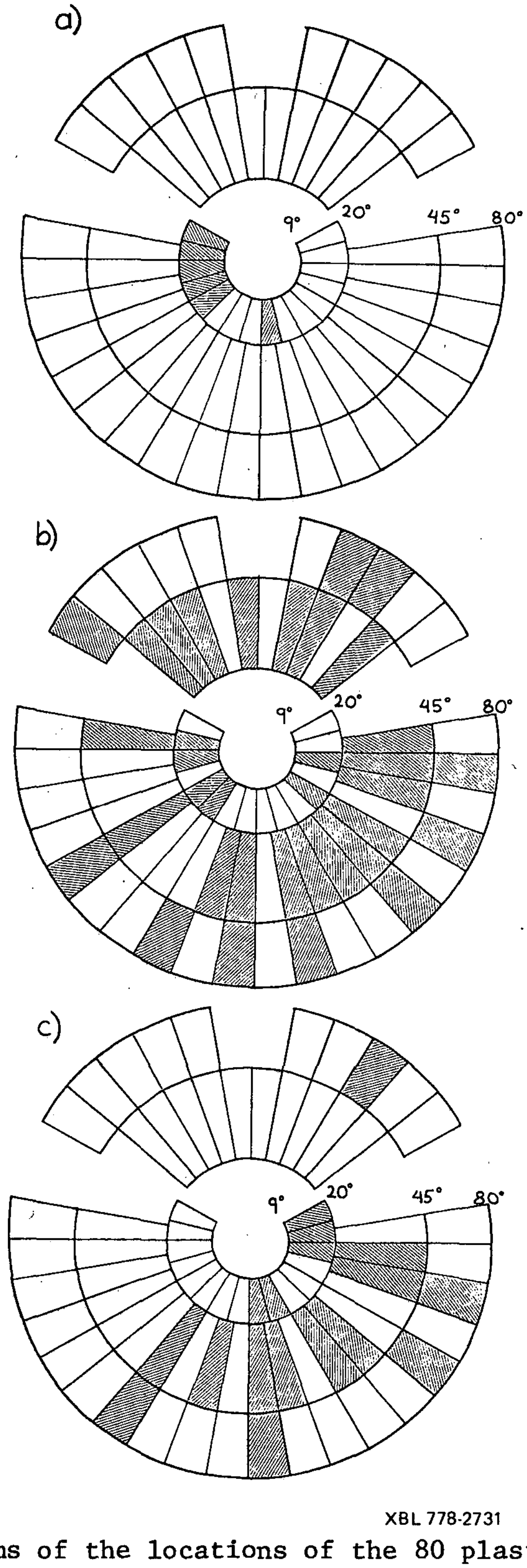


Fig. 11. Diagrams of the locations of the 80 plastic scintillators looking down the beam line. In these three events the shading indicates which plastic scintillators fired in coincidence with the telescope, which is at 90° to the beam on the right-hand side of the figure.

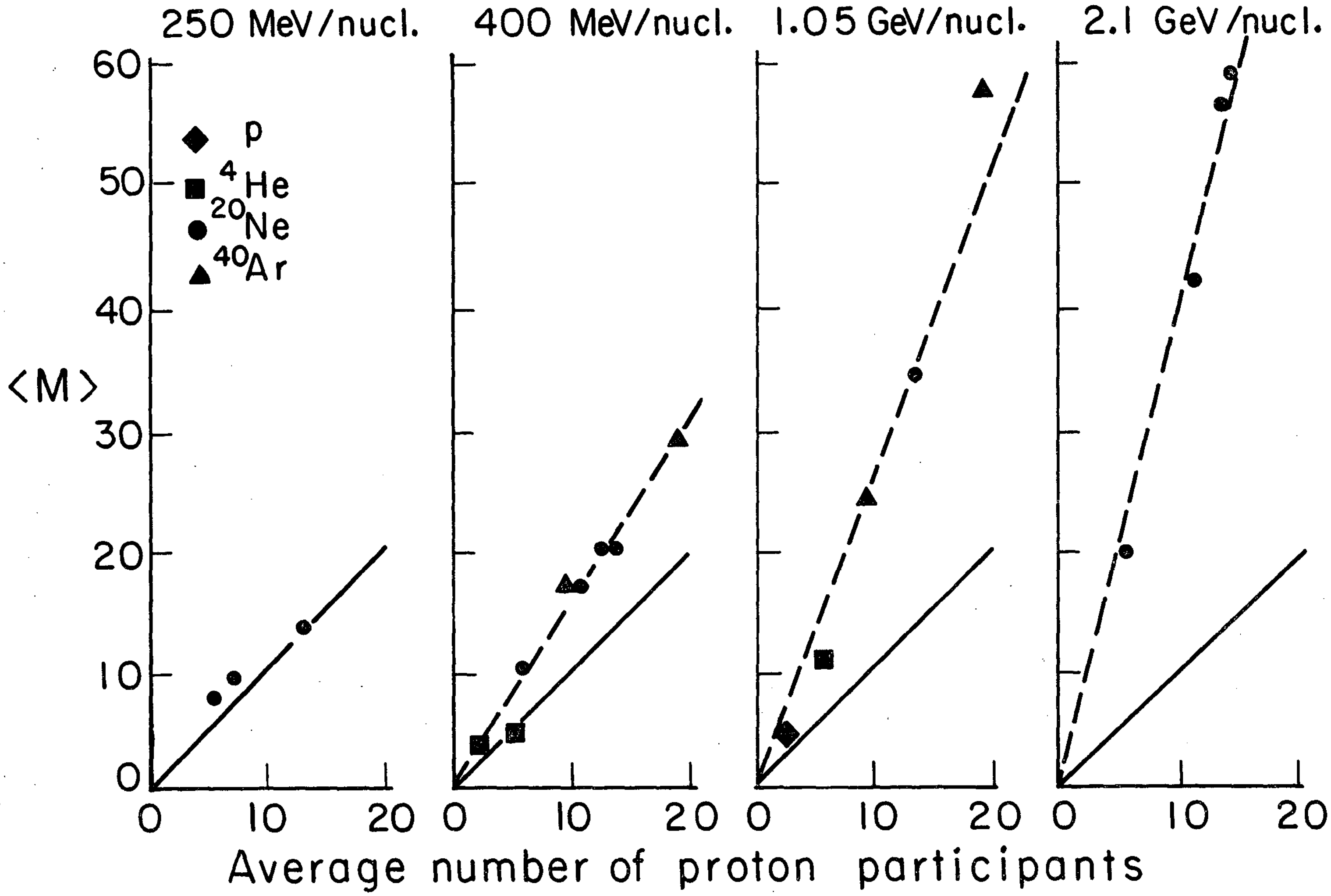


Fig. 12. The average multiplicity obtained from the scintillation paddles plotted vs. the average number of proton participants calculated from the fireball geometry. These are multiplicities associated with a proton in the telescope at 90° to the beam. Data from many different target-projectile combinations are shown at four bombarding energies. The dashed lines are through the data. The solid lines are drawn at 45° to represent the results expected from the fireball geometry. (XBL 787-1322)

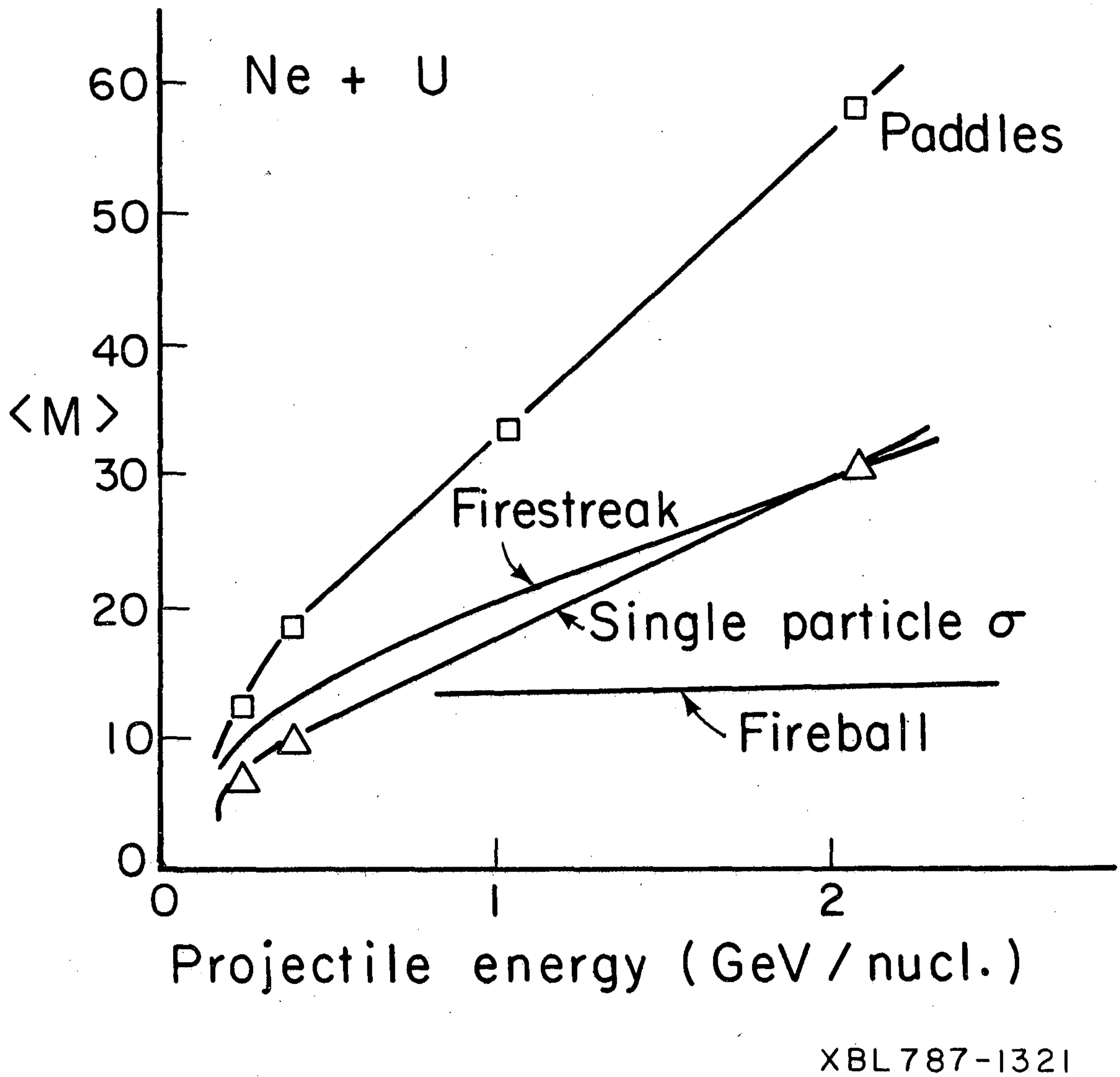


Fig. 13. The average multiplicities obtained in the paddles for the Ne plus U system as a function of the Ne projectile energy. Experimental results from the 80 paddles and the integrated single particle cross sections are shown. Also indicated are the calculations based on the fireball and firestreak models.

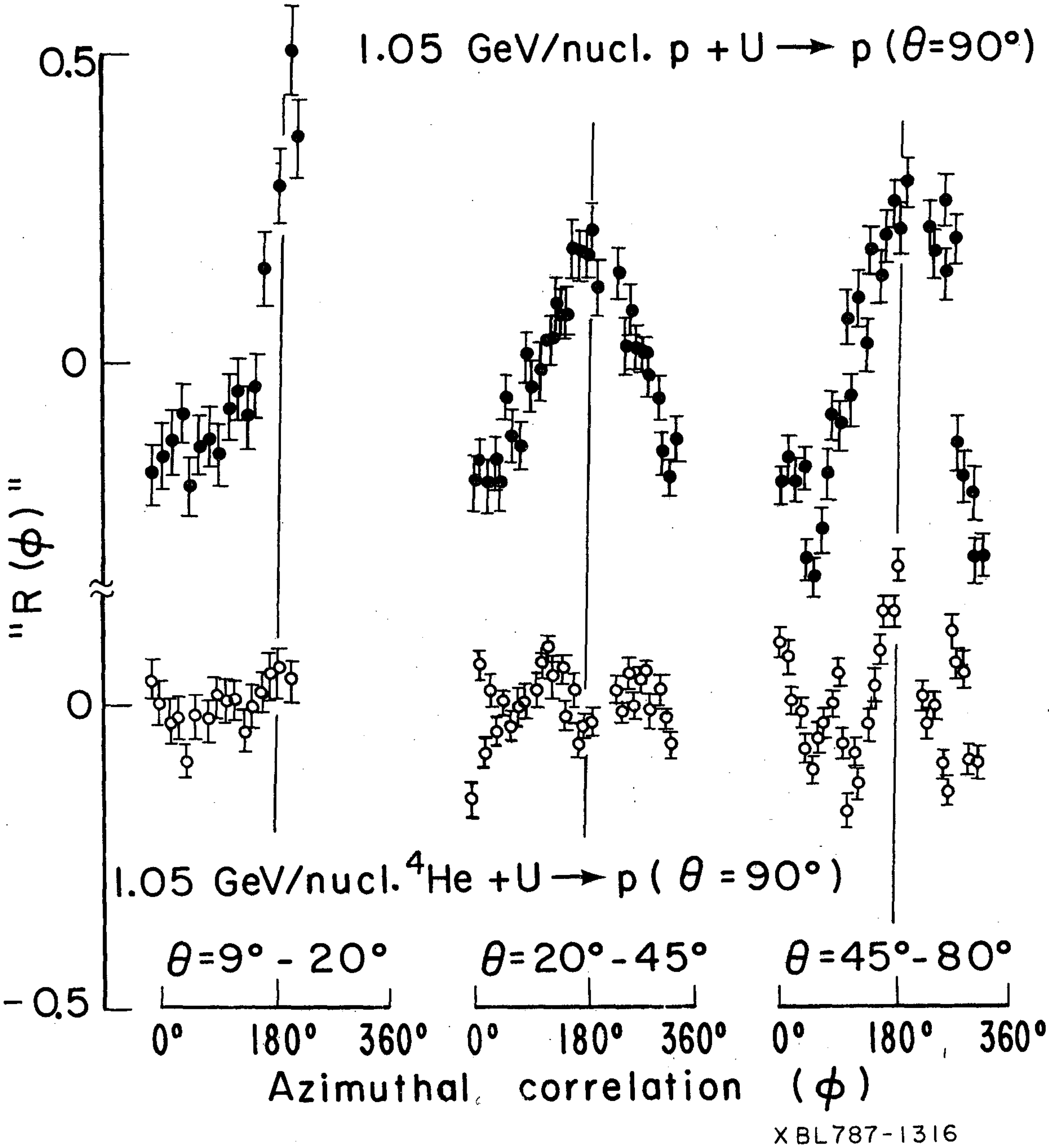


Fig. 14. Azimuthal correlations for three different polar angular intervals with respect to the beam. The correlations are with respect to a proton in the telescope at a θ angle of 90° to the beam and a φ angle of 0°. Shown above are the data for 1 GeV incident protons and below for 1 GeV/nucleon incident $^4$He ions.

This report was done with support from the Department of Energy. Any conclusions or opinions expressed in this report represent solely those of the author(s) and not necessarily those of The Regents of the University of California, the Lawrence Berkeley Laboratory or the Department of Energy.

TECHNICAL INFORMATION DEPARTMENT
LAWRENCE BERKELEY LABORATORY
UNIVERSITY OF CALIFORNIA
BERKELEY, CALIFORNIA 94720